JPE 11-2-15

Improvement in Computation of Δ V_{10} Flicker Severity Index Using Intelligent Methods

Payman Moallem†, Abolfazl Zargari*, and Arash Kiyoumarsi*

†* Dept. of Electrical Engineering, University of Isfahan, Isfahan, Iran.

Abstract

The ΔV_{10} or 10-Hz flicker index, as a common method of measurement of voltage flicker severity in power systems, requires a high computational cost and a large amount of memory. In this paper, for measuring the ΔV_{10} index, a new method based on the Adaline (adaptive linear neuron) system, the FFT (fast Fourier transform), and the PSO (particle swarm optimization) algorithm is proposed. In this method, for reducing the sampling frequency, calculations are carried out on the envelope of a power system voltage that contains a flicker component. Extracting the envelope of the voltage is implemented by the Adaline system. In addition, in order to increase the accuracy in computing the flicker components, the PSO algorithm is used for reducing the spectral leakage error in the FFT calculations. Therefore, the proposed method has a lower computational cost in FFT computation due to the use of a smaller sampling window. It also requires less memory since it uses the envelope of the power system voltage. Moreover, it shows more accuracy because the PSO algorithm is used in the determination of the flicker frequency and the corresponding amplitude. The sensitivity of the proposed method with respect to the main frequency drift is very low. The proposed algorithm is evaluated by simulations. The validity of the simulations is proven by the implementation of the algorithm with an ARM microcontroller-based digital system. Finally, its function is evaluated with real-time measurements.

Key Words: ΔV10, Adaline, FFT, Flicker index, Power quality, PSO

I. Introduction

When the frequency of voltage fluctuations in a power system closes to stimulate the eye-brain response, human visual systems perceive changes in the emitted lights of a lamp. This phenomenon is defined as voltage flicker in power quality studies [1], [2].

Fluctuating loads, which cause load currents, change continuously and extremely. For example, electric arc furnaces and arc welders [3] can cause disturbances which result in voltage flickers in weak power systems and affect the illumination in nearby distribution areas.

Voltage flickers can cause problems in some system equipment. They can affect the starting torque, the slip and the starting current. They can also cause overloads in motors and generators and rises in temperature. In addition, they can reduce the life of electronic devices, incandescent and fluorescent lamps and CRT devices. Electronic controllers are likely to operate incorrectly during voltage variations. They also influence the visual perception of light [4].

Light flicker is defined as the impression of fluctuations in brightness or color. Whether the human eye detects flicker at a given frequency depends on several conditions, including the light fixture, intensity, time variation, age, eye condition, emotional state and adaptation to background light [5]. Traditionally, if a certain level of flicker frequency is detected by 50% of a tested population, light flicker is said to occur.

When a flickering light source is passed to the eye, the dilator and sphincter muscles will alternatively dilate-contract. This can result in muscle fatigue and annoyance. Additional side effects may include headaches, eye strains and, in some cases, seizures [6], [7].

Methods of measurement to determine the severity of flicker would allow utilities to estimate its impacts on end-users and the power system. It would also provide information for selecting an appropriate mitigation technique since numerous options are available. In the last decade, many researchers have been involved in studies related to flicker measurement [8]–[11].

Two typical flicker meters are the UIE/IEC standard meter and the so-called equivalent 10 Hz voltage flicker (or ΔV_{10}) meter. ΔV_{10} is a measure widely used in Japan and in other Asia Pacific countries. In this paper, we will discuss the ΔV_{10} method and the disadvantages of employing the FFT (fast Fourier transform) algorithm to extract the frequency components from the flicker component. Then, a new method with high accuracy and a low computational cost is proposed. Some intelligent methods including the Adaline (adaptive linear neuron) and PSO (particle swarm optimization) are also used. When using Adaline, the envelope of the power system voltage (flicker components) is extracted. Therefore the sampling frequency, the computational cost and the request memory are effectively reduced when compared with con-

Manuscript received Aug. 8, 2010; revised Jan. 30, 2011
† Corresponding Author: p_moallem@eng.ui.ac.ir
Tel: +98-311-7934066, Fax: +98-311-6682887, University of Isfahan
* Dept. of Electrical Eng., University of Isfahan, Iran

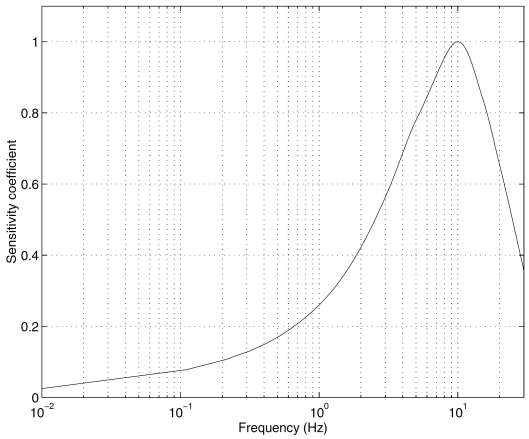

Fig. 1. Visual sensitivity curve [12].

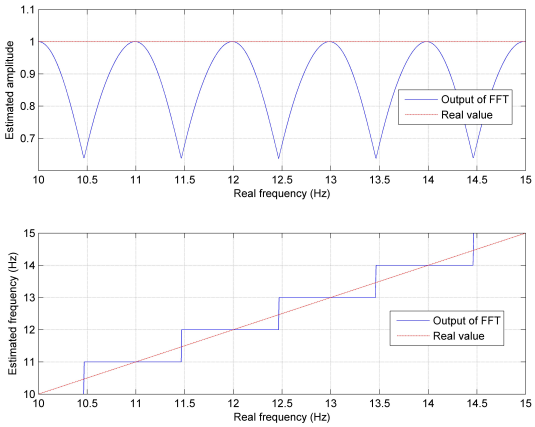

Fig. 2. Comparing the outputs of FFT and real values.

ventional FFT computation. When using the PSO algorithm, the real values of the amplitude and frequency of the flicker components are estimated with very little error. It is so accurate that it is not necessary to consider a large time window for the proposed method and as a result the computational cost and the request memory are reduced again. Indeed, the Adaline sustem reduces the computational cost and request memory, while the PSO algorithm reduces both the computational cost and the request memory and increases accuracy.

The proposed method has been implemented with an ARM microcontroller-based digital system and its function has been evaluated in practice.

In the next section, a brief review of the ΔV_{10} index and its measurements are introduced. Secondly, a spectral leakage error in FFT computation which affects the ΔV_{10} index computation is discussed. Then, the proposed improvement for ΔV10 flicker index computation using Adaline and PSO is presented and evaluated by simulations. Finally, an ARM microcontroller-based implementation and some experimental results are presented.

II. ΔV_{10} Flicker Index

One flicker index used in Japan and some other Asian countries is the "Equivalent 10-Hz Voltage Flicker (ΔV_{10})," published by the Central Research Institute of the Electric Power Industry (CRIEPI) of Japan in 1978 [12]. This institute developed a visual sensitivity curve based on a series of experimental results as illustrated in Fig.1. In Taiwan, ΔV_{10} is the method currently used by the Taiwan Power Company.

Since the 10Hz voltage flicker is found to cause the most discomfort for human eyes, the weighting value for the 10 Hz component of a signal is set to one, while the other values are set to less than one.

The FFT and other signal processing techniques can be employed to extract the frequency components of periodic and stochastic signals. When the amplitude of the voltage variation (denoted as Δv_n) for a component with n Hz is obtained, the next step is to find the equivalent effect of all of the frequency components with respect to 10 Hz as follows:

$$\Delta V_{10} = \sqrt{\sum_{n=1}^{\infty} (a_n . \Delta v_n)^2} \qquad (1)$$

where, a_n is the weighting value for the n-th component. Normally, frequencies are considered up to 30 Hz. On the basis of the CRIEPI experiment in Taiwan, in order to have a flicker free voltage, the measured ΔV_{10} is should be lower than 0.45%.

The FFT is often applied to extract the frequency components of periodic or aperiodic flickers [13], [14]. In addition to the FFT method, the continuous wavelet transform and Kalman filtering are also utilized to extract the frequency components of voltage flicker [15], [16]. Unfortunately, they remarkably increase the calculation load when compared to the FFT. However, the FFT results seem doubtful due to the effect of its spectral leaking error.

Equation (1) is the form that the equivalent eddy currents remain in. Since the equivalent eddy currents cannot be directly detected, the equivalent eddy currents should be eliminated by succeeding manipulations.

III. Disadvantages of Applying the FFT

When the ΔV_{10} flicker index is computed by the FFT algorithm, the results seem doubtful because of the possible leakage error and the picket fence effect of the Fourier transform [17]. In order to understand the disadvantages of the FFT a voltage component is considered as follows:

$$v(t) = 1.0\cos(2\pi f t) \qquad (2)$$

where, f is the frequency of the component and its amplitude is set to one. Assume that f changes linearly in the range of (10-15) Hz and that the FFT computation is applied on the voltage component. The frequency of the sampling and the timing window (T_w) are considered to be 500 Hz and one second, respectively. In Fig. 2, the outputs of the FFT (the solid line) and the real values (the dashed line) are shown.

As can be seen, the amplitude and frequency estimated by the FFT is slightly different than the real values. For example the obtained amplitude of a signal with a 10.5 Hz frequency is 0.65 which indicates a 35% variation toward the real amplitude.

The estimated frequency is also equal to 11 Hz which indicates a 0.5 Hz estimation error. Generally, it can be said that only components such as the 10 Hz component, where their frequency is an integral multiple of the frequency

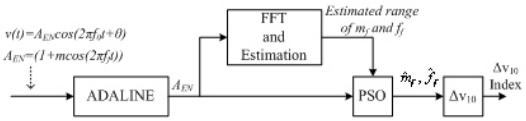

Fig. 3. Block diagram of the proposed method.

resolution ($1/T_w$), are well estimated by the FFT. In terms of the other components, only a range of their amplitude and frequency might be estimated. For example, if the output frequency of the FFT is 11 Hz, it can be estimated that the real frequency is in the range of 10.5 Hz to 11.5 Hz and that the real amplitude is in the range of 0.6 to 1.

Some approaches for improving the FFT transform have been proposed such as flat-top windows [18], adjustable window [19], interpolating windowed [20], and so on. Usually, in an effort to imporve the FFT transform, the rectangular window is replaced by windows such as the Hanning, the Hamming, the Kaiser, or the flat-top [21]. Although, the spectral leakage problem is small the picket fence effect still exists. Therefore, errors in amplitude and frequency measurements still exist. Moreover, output results depend on the length of window and it requires a large amount of memory and high computational cost.

In this paper, a new method is proposed to reduce the computational cost and the error of the FFT calculations. With this method, instead of the voltage amplitude, its envelope is evaluated, which results in a reduction of the total memory and the computational cost because it reduces the sampling frequency. Moreover, for increasing the accuracy in computing the flicker components, the PSO optimization algorithm is used to reduce the spectral leakage error in the FFT calculations.

IV. The Proposed Method

A block diagram of the proposed ΔV_{10} measurement method is shown in Fig. 3.

In the proposed method, first the envelope of the power system voltage (A_{EN}), which contains the flicker component, is extracted by the Adaline system and then the FFT is implemented on the output of the Adaline.

Using the envelope of the power system voltage to extract the flicker component reduces the computational cost and the sampling memory. Moreover, the sampling frequency is reduced. The output of the FFT block estimates the range of the frequency and amplitude of the flicker component that is given to the PSO block.

The POS block tries to estimate the real values of the amplitude and frequency of the flicker components with very little error. The estimated values of the frequency and the corresponding amplitude are converted to the ΔV_{10} flicker intensity index by the ΔV_{10} block in Fig. 3. The next sections present the functions of each block in detail.

A. Flicker Voltage Identification

According to equation (3), interhormonics with f_{IH} frequency make a flicker with a frequency of f_f:

$$f_f = |f_{IH} - f_0| \tag{3}$$

where, f_0 is the main harmonic of the system and f_{IH} is within a 30 HZ interval of the main harmonic and therefore f_f is within the interval from 0 Hz to 35 Hz. In general, the effect of the interharmonic components on the voltage of a power system can be expressed as an amplitude modulated (AM) signal as follows [22], [23]:

$$v(t) = \left[A_0 + \sum_{i=1}^{m} \{A_f \cos(2\pi f_f t + \phi_f\}\right] \cos(2\pi f_0 + \phi_0) = A_{EN} \cos(2\pi f_0 + \phi_0) \tag{4}$$

where,
A_0 is the fundamental voltage amplitude.
f_0 is the power frequency.
A_f is the amplitude of the flicker voltage.
f_f is the flicker voltage frequency.
m is the number of flicker modes.
ϕ_f is the phase angle of the flicker voltage.
ϕ_0 is the phase angle of the main harmonic.

Therefore, by extracting the envelope A_{EN} of an AM signal, the flicker components are identified. To evaluate the envelope A_{EN} of an AM signal, many methods have been proposed such as squaring demodulation, discrete wavelet synchronous detection, an enhanced phase-locked loop [24], a Kalman filter [25], and the Hilbert transform [26]. One of the methods is Adaline detection, which has a simple calculation.

B. Adaline Block

An Adaline is a single layer neural network with multiple nodes, one output and several adjustable weights [27]. The objective of using an Adaline system is to extract the envelope of the power system voltage which effectively reduces the computational cost and the memory used in FFT computation. When the FFT is directly implemented on a signal, it is necessary to sample the signal with a sampling frequency much higher than the frequency of the signal and the memory used in the time-window needs to be sufficiently large. In the proposed method, the Adaline weights are adjusted such that it tries to track the envelope of the power system voltage.

In order to explain the function of the Adaline algorithm, equation (4) is implemented as equation (5):

$$\begin{aligned} v(t) &= (A_{EN} \cos(\phi_0)) \\ &\cos(2\pi f_0 t) - (A_{EN} \sin(\phi_0)) \sin(2\pi f_0 t) \\ &= w_1 x_1 + w_2 x_2 \end{aligned} \tag{5}$$

where, the weights w_1 and w_2 denoting $(A_{EN}\cos(\phi_0))$ and $(-A_{EN}\sin(\phi_0))$ are the parameters of the adaptive filter, respectively. The so called reference signals x_1 and x_2 are built according to the nominal angular frequency as $\cos(2\pi f_0 t)$ and $\sin(2\pi f_0 t)$. The proposed Adaline system is shown in Fig. 4, where, $v(t)$ is the measured power system voltage, $\hat{v}(t)$ is the output of the Adaline system and $e(t) = v(t) - \hat{v}(t)$ is the prediction error at time t. The weighting coefficients are adjusted based on the error signal and an adaptation rule. When $e(t)$ becomes zero, it can concluded that the measured voltage A_{EN} is [28]:

$$A_{EN} = \sqrt{w_1^2 + w_2^2} \tag{6}$$

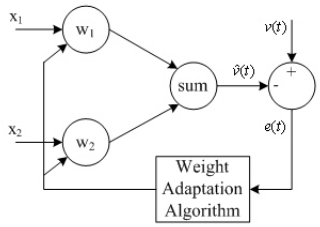

Fig. 4. Adaline block diagram for envelope tracking system.

In the Adaline neural network, the least mean square (LMS) algorithm, known as the Widro-Hoff delta rule, is usually used as an adaptation rule. For the k-th sample, the adaptation rule is given by [28]:

$$W(k+1) = W(k) + \alpha \frac{X(k)e(k)}{X(k)^T X(k)} \tag{7}$$

where, $X(k)$ is the k^{th} sample of the input vector, $e(k)$ is the error signal for the k^{th} sample and α is the learning rate.

C. FFT and the Estimation Block

In this block, the FFT algorithm is implemented on the flicker component (A_{EN}) that was made from the previous block. If $v(t)$ in equation (4) has no flicker, it means that A_{EN} is constant and the FFT of A_{EN} has only one nonzero component at the zero frequency. For nonzero frequencies less than 30Hz based on the ΔV_{10} standard (Fig. 1), suppose that the maximum amplitude and the corresponding frequency are m_m and f_m, respectively. When m_m is larger than the predefined value β, there is a flicker in $v(t)$ (equation (4)). The β value depends on the real amplitude of $v(t)$. The range of the frequency and the corresponding amplitude of the flicker component (f_{f_Range}, m_{f_Range}), which are used in the following PSO block, can be estimated by equation (8):

$$\begin{aligned} f_f - \frac{1}{T_W} \le f_{f\_Range} \le f_f + \frac{1}{T_W} \\ m_m \le m_{f\_Range} \le m_m + \gamma m_m \end{aligned} \tag{8}$$

where, T_w is the timing window and γ is a constant less than 1.0.

D. PSO Block

The PSO algorithm, which is in the class of evolutionary algorithms, was proposed by Kennedy and Eberhart in 1995 [29]. These types of optimization algorithms have been increasingly applied for optimizing power system problems in recent years [30]. The PSO algorithm is a set of particles (the optimization variables) that diffuse in the search space. Each particle may be a potential solution. It is obvious that some particles have a better position than other particles and that the rest try to promote their position to a superior particle's position. At the same time, the superior particle's position also changes. The change in each particle's position is based on the particle's experience in the previous movements and the neighboring particle's experience. Indeed, each particle is aware of its superiority and non-superiority toward the neighboring particles and also toward the total group.

In order to explain the function of the PSO algorithm in this paper, it is assumed that the estimated flicker component of the PSO algorithm is as:

$$\hat{A}_{EN} = \left[A_0 + \sum_{i=1}^{m} \{ \hat{A}_f \cos(2\pi \hat{f}_f t + \hat{\phi}_f \} \right]. \tag{9}$$

In each moment of the k^{th} sample, the difference between the real flicker component and the estimated component is provided to the algorithm and according to the objective function and the range of the optimization variables which are obtained by the FFT algorithm, the best estimation is computed. Since the range of the optimization variables is very small, the algorithm estimates the variables at an appropriate speed and results in a very good estimation.

In the PSO algorithm, the particles search for the best positions until a relatively unchanging state has been encountered or until the computational limitation exceeded. The PSO concept consists of changing the velocity of each particle toward its *pbest* and *gbest* positions at each time step. The velocity is weighted by a random term, with separate random numbers generated for velocity toward the *pbest* and *gbest* positions. The process of PSO can be described as follows:

1. Initialize a population (array) of particles with random positions and velocities in d dimensions in the problem space.
2. For each particle, evaluate the desired optimization fitness function in d variables.
3. Compare a particle's fitness evaluation with its *pbest*. If the current value is better than *pbest*, then set the *pbest* position equal to the current position in d dimensional space.
4. Compare the fitness evaluation with the population's overall previous best. If the current value is better than *gbest*, then reset *gbest* to the current particle's array index and value.
5. Change the velocity and position of the particle according to equation (11) and (12) respectively:

$$\begin{aligned} v_i^{k+1} = w v_i^k + c_1 rand(.)(pbest - x_i^k) \\ + c_2 rand(.)(gbest - x_i^k) \end{aligned} \tag{11}$$

$$x_i^{k+1} = x_i^k + v_i^{k+1} \tag{12}$$

where, v_i^k, v_i^{k+1} and x_i^k are the velocity vector, the modified velocity and the positioning vector of particle i at generation k, respectively. c_1 and c_2 are the cognitive and social coefficients that influence particle velocity. In these equations, it should be noted that the largeness of v_{max} may make the particles pass over the minimum-point and the smallness may make the particle rotate around its position so that it can not search the testing space. The amount of v_{max} is typically selected from between 10 to 20 percent of the range of the variables. Besides, an appropriate selection of w results in the algorithm being repeated less to achieve the optimized point. In typical PSO algorithms the coefficient w reduces from 0.9 to 0.4 while implementing the algorithm and it is reduced according to the following equation:

$$w = w_{\max} - \frac{w_{\max} - w_{\min}}{iter_{\max}} . \; iter \tag{13}$$

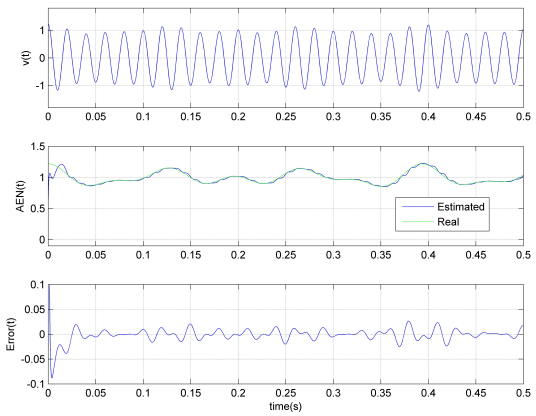

Fig. 5. The curves of $v(t)$, output of Adaline, and error signal.

Another problem in implementing this algorithm is to select appropriate values for c_1 and c_2. In many algorithms, the values of c_1 and c_2 are selected in a way that $c_1 + c_2 \leq 4$.

6. Return to step 2 until a criterion is met, usually a sufficiently good fitness or a maximum number of iterations (generations).

E. ΔV_{10} Block

In this block, according to the ΔV_{10} method, the ΔV_{10} flicker index can be computed by Equation (1) and the output data of PSO block.

V. Evaluation of the Proposed Method

It is assumed that the measured signal $v(t)$ is as follows:

$$\begin{aligned} v(t) &= A_{EN}(t)\cos(2\pi 50t + \pi/3) \\ A_{EN}(t) &= 1 + 0.1\cos(2\pi 7.6t) \\ &+ .05\cos(2\pi 10.1t) + .07\cos(2\pi 15.3t) \end{aligned} \quad (14)$$

which has a main component of 50 Hz frequency and an amplitude equal to 1.0 together with flicker components of 7.6, 10.1, 15.3 Hz frequency and 10, 5, 7 % amplitudes, respectively. The frequency of the sampling and the timing window are considered equal to 200 Hz and 4 second, respectively. This voltage is applied to the proposed algorithm and the output of each block will be discussed.

A. Adaline Block

The Adaline neural network (Fig. 5) with x_1 and x_2 equal to $\cos(2\pi 50t)$ and $\sin(2\pi 50t)$, respectively, is used to extract the envelope of $v(t)$ in equation (14). The Adaline neural network is trained based on equation (7) with initializing values for the weight parameters (w_1 and w_2) and a learning rate (α) set to zero and 0.5, respectively. The curves of $v(t)$, the output of Adaline (A_{EN} in equation (14)), and the error signal are shown in Fig. 5, respectively.

The results show that the Adaline system has successfully estimated the voltage envelope (A_{EN} in equation (14)) and that the error is small.

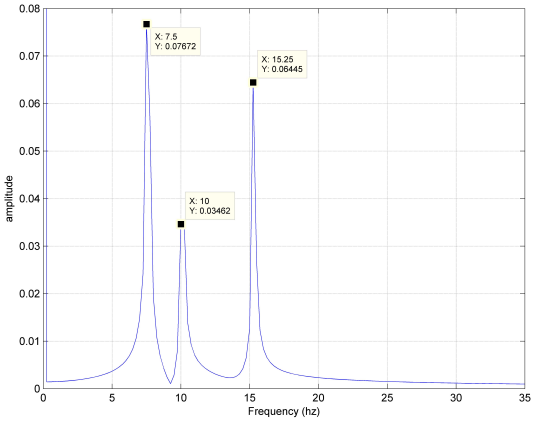

Fig. 6. Frequency spectrum of A_{EN} signal.

TABLE I
The Range of m_f and f_f

	Range of m_f	Range of f_f (Hz)
Component 1	(0.0766,0.1302)	(7.25,7.75)
Component 2	(0.0345,0.0586)	(9.75,10.25)
Component 3	(0.0644,0.1094)	(15,15.5)

B. FFT and the Estimation Block

The amplitude of the Fourier transform of the voltage envelope (A_{EN}), which is calculated by the FFT block, is shown in Fig. 6. For the measured signal $v(t)$ in equation (14), the value of β is set to 0.01.

Considering equation (8) with $\gamma = 0.7$ and $T_w = 4.0$ seconds, for frequencies higher than zero but less than 30 Hz, based on the ΔV_{10} standard (Fig. 1), the FFT block estimates the presence of flicker components in the ranges in Table I.

It can be seen that the FFT block can only estimate a range of flicker parameters and that it is necessary to determine an accurate values for the flicker components which are calculated by the following PSO block.

C. PSO Block

The PSO input parameters are considered to be, $c_1 = c_2 = 2$, $w_{min} = 0.4$, $w_{max} = 0.9$, iteration= 30, number of particles= 50. The output of the PSO block estimates the parameters of the flicker component as shown in Table II.

D. Generally Evaluating

In order to generally evaluate the effects of the flicker frequency on the proposed algorithm, A_{EN} is considered to be:

$$A_{EN} = 1 + 0.1\cos(2\pi f_f t). \quad (15)$$

It is assumed that f_f is a variable along 10 to 15 Hz. The frequency of the sampling and the timing window are considered to be equal to 200 Hz and 4 second, respectively. Comparisons of the outputs of the PSO and the real values are shown in Fig. 7.

The results show both the frequency and the amplitude of the flicker component. The average values of the errors are 5.84×10^{-4} and 1.61×10^{-5} for the frequency and amplitude of the flicker component, respectively.

TABLE II
THE ESTIMATED VALUES OF m_f AND f_f

	Estimated of m_f	Estimated f_f (Hz)
Component 1	0.09998	7.598
Component 2	0.050005	10.001
Component 3	0.06999	14.9997

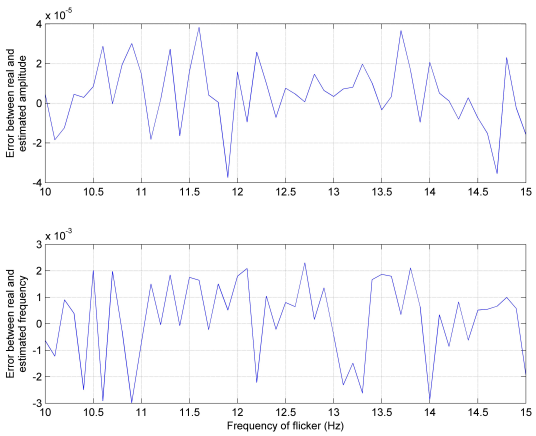

Fig. 7. Error between the outputs of the proposed method and real values in different flicker frequencies.

E. Comparison

In Fig. 8, a comparison between the proposed method and the conventional FFT method for calculating the ΔV10 index is shown. A_{EN} is considered in equation (15) and it is assumed that f_f is a variable around 0 to 35 Hz with step size of 0.005 Hz.

In the proposed method, the frequency of the sampling and the timing window are considered to be equal to 200 Hz and 4 seconds, while in the conventional FFT method, the frequency of the sampling and the timing window are considered to be equal to 700 Hz and 60 second, respectively. Therefore, the request memory in the conventional FFT method is 53 times larger than in the proposed method. The results in Fig. 8 also show that the proposed method has a very small error when compared to the conventional FFT method. The average values of the errors for the proposed and conventional FFT methods are 2.32×10^{-4} and 0.0405, respectively. Moreover, using the Matlab 2008 environment with a 3.0 GHz AMD dual-core CPU, the calculation times for the ΔV_{10} index in the proposed and conventional FFT methods are 0.0638 and 0.1075, respectively.

VI. EFFECTS OF THE MAIN FREQUENCY DRIFT

To describe and implement the Adaline system, it is assumed that the main frequency of the power system is 50Hz while sometime it may be more or less than this value. Therefore, it is essential to evaluate the function of the Adaline system and then the whole of the proposed algorithm. It is assumed that the main frequency of the system has drifted to 45Hz and that the measured signal $v(t)$ is as equation (16):

$$\begin{aligned} v(t) &= A_{EN}\cos(2\pi 45t+\pi/3) \\ A_{EN} &= 1+0.1\cos(2\pi 7.6t) \\ &+.07\cos(2\pi 15.3t)+.05\cos(2\pi 10.1t) \end{aligned} \tag{16}$$

The frequency of the sampling and the timing window are considered equal to 200 Hz and 4 seconds, respectively. The

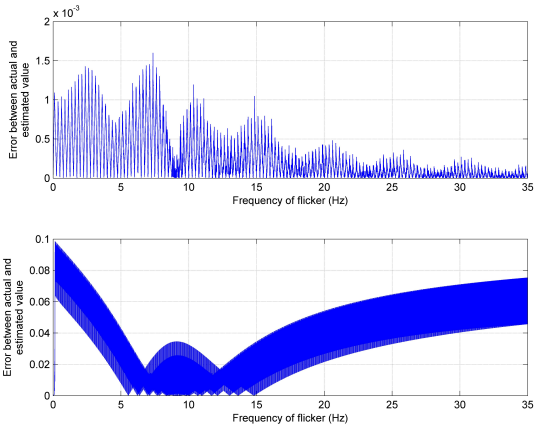

Fig. 8. Error between actual and estimated value of ΔV_{10} index. (a) The proposed method. (b) The conventional FFT method.

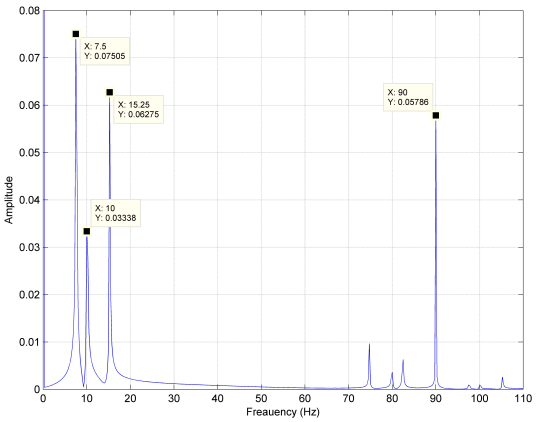

Fig. 9. Frequency spectrum of A_{EN} signal.

estimated envelope consists of two frequencies, the low frequency which is the flicker frequency and the high frequency which is created based on reducing the main frequency. The second frequency which can be considered as an error in the estimated envelope, is also increased by increasing the difference between the real main frequency and the predefined main frequency, 50Hz. The amplitude of the Fourier transform of the voltage envelope (A_{EN}) which is calculated by a FFT block is shown in Fig. 9.

In this case, the FFT and the estimation algorithm estimate the presence of flicker component in the interval from 0 Hz to 30 Hz. The range amplitude and frequency of the flicker can be computed based on equation (8). The output of a PSO block can also estimate the parameters of the flicker component accurately, as shown in Table III.

As can be seen, the proposed algorithm is resistant to frequency shifts and it estimates appropriate values well. When the FFT and other methods, such as the wavelet and kalman filter methods, are directly implemented on a signal, it is necessary, for detecting the flicker component and based on Equation (3), to detect the interharmonic component and the main harmonic component. However, in the proposed method this is not necessity, even with existence of main harmonic drift. It is another advantage of the proposed method.

In order to generally evaluate the effects of change in the main frequency on the proposed algorithm, A_{EN} is considered

TABLE III
THE ESTIMATED VALUES OF m_f AND f_f

	Estimated of m_f	Estimated f_f (Hz)
Component 1	0.0991	7.5905
Component 2	0.0506	9.983
Component 3	0.0690	14.979

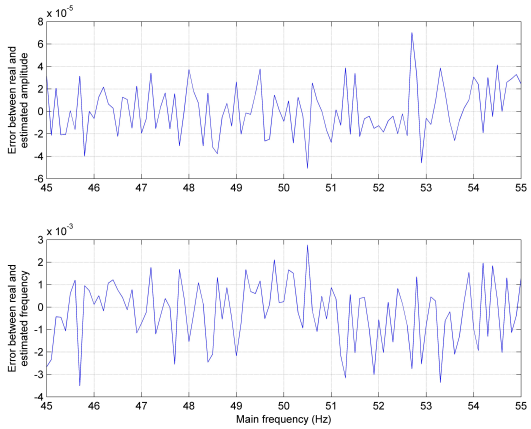

Fig. 10. Error between the output of the proposed method and real values in different main frequency.

as:

$$v(t) = A_{EN}\cos(2\pi f_0 t + \pi/3)$$
$$A_{EN} = 1 + 0.1\cos(2\pi 10.1 t). \quad (17)$$

It is assumed that f_0 is a variable about 45 to 55 Hz. The frequency of the sampling and the timing window are considered to be equal to 200 Hz and 4 second, respectively. Comparisons of the outputs of the PSO and the real values are shown in Fig. 10.

Based on Fig. 10, the average values of the errors are 5.91×10^{-4} and 1.75×10^{-5} for the frequency and amplitude of the flicker component, respectively. This means that, even if the main frequency of the system is varied, the errors in the estimation of the frequency and amplitude of the flicker component are very low.

VII. IMPLEMENTATION OF THE PROPOSED METHOD

In this section, a practical implementation of the proposed method is presented. In a practical implementation, the amount of RAM memory and the computational ability of the system play essential roles. A powerful processor is needed to implement the FFT, the Adaline and other parts of the proposed method. Sufficient ROM memory (for programs and fixed data) and sufficient RAM memory (for FFT and the other variables) are also required. Moreover, the execution time should be low. The proposed method was designed and implemented by an experimental digital system based on an ARM microcontroller [31] LPC2368 that includes 512KB of ROM, 48KB of RAM and a clock frequency equal to 72MHz.

The whole of experimental system is shown in Fig.11. It includes the ARM microcontroller, the programming interface, the input analog interface, which is connected to the 10 bit A/D converter of the ARM, and an LCD display to report the flicker measurements.

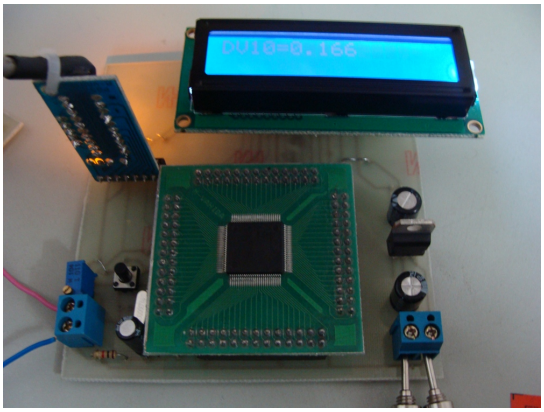

Fig. 11. An experimental flicker meter based on an ARM microcontroller.

TABLE IV
THE EXECUTION TIME OF DIFFERENT PARTS OF THE PROPOSED METHOD IN ARM BASED SYSTEM

	Block 1	Block 4	Block 6
Execution Time	4.00	0.90	2.85

A. ARM-based flicker meter

There is a tradeoff between the sampling time, the sampling frequency and the accuracy of the system. The frequency resolution of the FFT algorithm, which is used for extracting the flicker components, is an important parameter when the ΔV_{10} method is digitally implemented. In order to reach an acceptable frequency resolution of about 0.25Hz, the sampling window is set to 4 seconds and the sampling frequency is set to 200 Hz, based on the available RAM memory. Fig. 12 shows a flowchart of the program, which is written in C language and compiled with a Keil compiler. The sampling frequency is adjusted by one of the ARM timers.

The execution time of the proposed algorithm which is written in C language is about 7.75 second on the experimental ARM based system. This means that after connecting the system to a power line, the ΔV_{10} flicker severity index is available in less than 8 seconds. Table IV shows the partial execution time of the main blocks of the flowchart in Fig. 12, including the sampling (block 1), the FFT computation (block 4) and the PSO (block 6). The execution times of the other blocks are negligible. The Adaline computation (block 3) is executed in the sampling time. While the ΔV_{10} index computation of a 4 second window is done, the next window is sampled. Therefore, data acquisitions are done without interruption and the output is updated every 4 seconds.

B. Practical Tests

In this subsection, the results of practical experiments on manipulated flicker meters are presented. In all of the experiments, a signal generator is used to generate $v(t)$ as:

$$v(t) = A_{EN}(t)\cos(2\pi f_0 t)$$
$$A_{EN}(t) = 1 + A_f\cos(2\pi f_f t) \quad (18)$$

where, f_0 is the main frequency of 50Hz and $A_{EN}(t)$ is the variation of $v(t)$ due to a flicker with an amplitude of A_f and a frequency of f_f.

Table V shows the results of five experiments including the amplitude and frequency of the flickers, the true ΔV_{10}

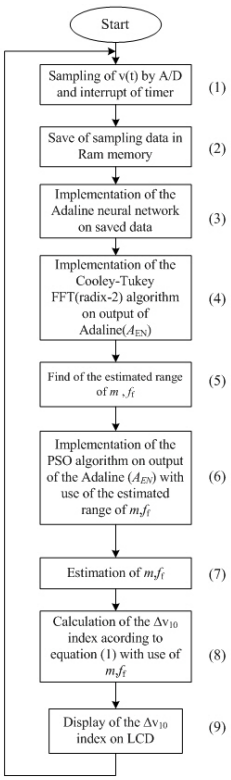

Fig. 12. The flowchart of implementation of the proposed method in experimental system based on ARM microcontroller.

TABLE V
THE RESULTS OF FIVE EXPERIMENTS IN ARM BASED SYSTEM

Experiment	Flicker Characteristics		True ΔV10 Index	Measured ΔV10 Index	Relative Error
	A_f	f_f			
First	0.20	5 Hz	0.16	0.158	1.25 %
Second	0.10	10 Hz	0.1	0.103	3.00 %
Third	0.2	15 Hz	0.168	0.166	1.20 %
Fourth	0.05	20 Hz	0.0325	0.030	7.69 %
Fifth	0.30	25 Hz	0.15	0.148	1.33 %

index and the corresponding measured ΔV_{10} index by the manipulated flicker meter, as well as the percentage of relative error.

In this practical test, flicker frequencies between 5 to 25 Hz were covered and the relative error of the manipulated system was investigated. The error was less than 7.7% in the worst case and the average was less than 2.9%.

In order to investigate the operation of the Adaline envelope detector, one of the DACs of the ARM microcontroller was driven by the output of the Adaline envelope detector. For the second experiment in Table V, Fig. 13 shows the DAC output, which is the envelope of the signal, by a 20 MHz traditional oscilloscope.

Fig. 14 shows the measured ΔV_{10} index for the third experiment in Table V, where the true value of the ΔV_{10} flicker index is 0.168.

VIII. CONCLUSIONS

The ΔV_{10} flicker severity index as a common method of flicker metering can be computed by the FFT computation of a sampled voltage with a sufficient sampling frequency and

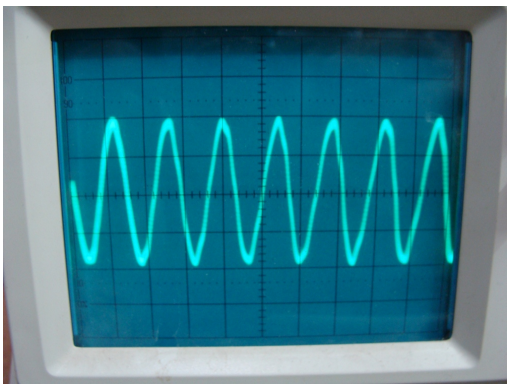

Fig. 13. The output of the Adaline envelope detector for the third experiment in Table V, where time/div is set to 50 msec. and volt/div is set to 0.1 volt. The base frequency is 50 Hz and the flicker amplitude and frequency is 20% and 15Hz, respectively.

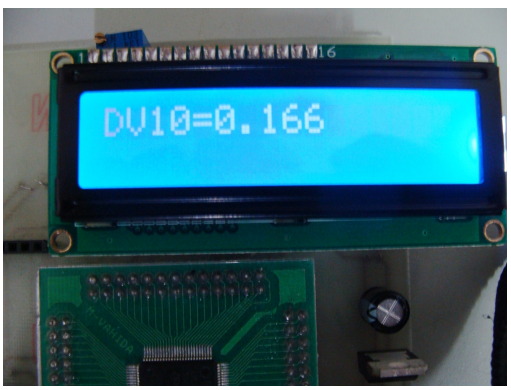

Fig. 14. The measured ΔV_{10} index for the third experiment in Table V, where the real ΔV_{10} index is 0.168 and the relative error is about 1.2%.

time. The direct implementation of the FFT on a sampled voltage suffers from the FFT disadvantages of a spectral leakage error and the picket fence effect. This paper presents a computational method for measuring the ΔV_{10} flicker severity index with a low computational cost and memory, using some intelligent methods. First, the envelope of the power system voltage is extracted by the Adaline neural network which is adjusted based on online voltage variations. Then by the FFT computation of the voltage envelope, a proper range for the frequency and magnitude of the flicker component are determined which are used in the PSO optimization to accurately determine the frequency and magnitude of the flicker component. Finally, the ΔV_{10} flicker severity index is computed based on the accurate frequency and magnitude of the flicker component.

The simulation results show that the error of the proposed method very small and that it requires less memory and a smaller sampling time. Moreover, the sensitivity of the proposed method with respect to variations in the system main frequency is negligible.

Finally a practical implementation of the proposed method is presented based on an ARM microcontroller with a sampling time of 4 second and a sampling frequency equal to 200 Hz. The execution time of the proposed method which is implemented in C language is less than 8 second for a LPC2378 with a clock frequency of 72 MHz. Experiments on the implemented flicker meter system shows that the average

of the relative error between the real and the measured ΔV_{10} flicker index is less than 2.9%. Therefore this system can be used as a low cost practical ΔV_{10} flicker severity measurement with an acceptable error.

REFERENCES

[1] G. Diez, L. I. Eguiluz, M. Manana, J. C. Lavandero, and A. Ortiz, "Instrumentation and methodology for revision of European flicker threshold," in *Proc. IEEE 10th International Conference on Harmonics and Quality of Power*, pp. 262-265, Oct. 2002.

[2] W. Xu, "Defeciency of the IEC flicker meter for measuring interharmonic-caused voltage flickers," in *Proc. IEEE Power Engineering Society General Meeting*, Vol. 3, pp. 2326-2329, Jun. 2005.

[3] A. Hernández, J. G. Mayordomo, R. Asensi, and L. F. Beites, "A Method Based on Interharmonics for Flicker Propagation Applied to Arc Furnaces," *IEEE Trans. Power Del.*, Vol. 20, No. 3, Jul. 2005.

[4] T. Zheng and E. B. Makram, "Wavelet representation of voltage flicker," *Electric Power Systems Research*, Vol. 48, No.2, pp.133-140, Dec. 1998.

[5] A. E. Emanuel and L. Peretto, "A simple lamp-eye-brain model for flicker observations," *IEEE Trans. Power Del.*, Vol. 19, No.3, pp.1308-1313, Jul. 2004.

[6] N. A. Smith, *Lighting for Health and Safety, Butterworth-Heinemann*, Boston, MA, 2000.

[7] C. Wang and M. J. Devaney, "Incandescent lamp flicker mitigation and measurement," *IEEE Transactions on Instrumentation and Measurement*, Vol. 53, No. 4, pp. 1028-1034, Aug. 2004.

[8] S. Caldara, placeS. Nuccio, and C. Spataro, "A virtual instrument for measurement of flicker," *IEEE Trans. Instrum. Meas.*, Vol. 47, No. 5, pp. 1155-1158, Oct. 1998.

[9] R. Arsenau, M. E. Sutherland, and J. J. Zelle, "A test system for calibrating flickermeters," *IEEE Trans. Instrum. Meas.*, Vol. 51, No. 4, pp. 598-600, Aug. 2002.

[10] S. J. Huang and C. W. Lu, "Enhancement of digital equivalent voltage flicker measurement via continuous wavelet transform," *IEEE Trans. Power Del.*, Vol. 19, No. 2, pp. 663-670, Apr. 2004.

[11] T. Keppler, N. Watson, and J. Arrillaga, "Computation of the short-term flicker severity index," *IEEE Trans. Power Del.*, Vol. 15, No. 4, pp. 1110-1115, Oct. 2000.

[12] *New trend in supply problems of arc furnace for steel plants*, Tech. report of Electrical engineering society (Japan), Vol. 2, pp. 3-26, 1978.

[13] C. J. Wu and T. H. Fu, "Effective voltage flicker calculation algorithm using indirect demodulation method," in *Proc. IEE Generation, Transmission and Distribution*, Vol. 150, No. 4, pp. 493-500, Jul. 2003.

[14] J.-L. Guan, J.-C. Gu, and C.-J. Wu, "Real-time measurement approach for tracking the actual coefficient of $\Delta V/\Delta V10$ of electric arc furnace," *IEEE Trans. Power Del.*, Vol. 19, No. 1, pp. 309-315, Jan. 2004.

[15] S.-J. Huang and C.-W. Lu, "Enhancement of digital equivalent voltage flicker measurement via continuous wavelet transform," *IEEE Trans. Power Del.*, Vol. 19, No. 2, pp. 663-670, Apr. 2004.

[16] N. Koose, O. Salor, and K. Leblebicioglu, "Interharmonics analysis of power signals with fundamental frequency deviation using Kalman filtering," *Electric Power Systems Research*, Vol. 80, No.9, pp. 1145-1153, Sep. 2010.

[17] Y.F. Li and K.F. Chen, "Eliminating the picket fence effect of the fast Fourier transform," *Computer Physics Communications*, Vol. 178, No.7, pp. 486-491, Apr. 2008.

[18] L. Salvatore and A. Trotta, "Flat-top windows for PWM waveform processing via DFT," *IEE Electric Power Applications*, Vol. 135, No. 6, pp.346-361, Nov. 1988.

[19] R. M. Hidalgo and J. G. Fernandez, R.R. Rivera, H.A. Larrondo, "A simple adjustable window algorithm to improve FFT measurements," *IEEE Trans. Instrum. Meas.*, Vol. 51, No. 1, pp.31-36, Feb. 2002.

[20] F. Zhang, Z. Geng, and W. Yuan, "The algorithm of interpolating windowed FFT for harmonic analysis of electric power system," *IEEE Trans. on Power Del.*, Vol. 16, No. 2, pp.160-164, Apr. 2001.

[21] G. Roberts, "A computationally efficient power-of-two window for spectral analysis," in Proceeding of *IEEE Aerospace Conference*, Vol. 4, pp. 221-230, 1998.

[22] O. Poisson, P. Rioual, and M. Meunier, "New signal processing tools applied to power quality analysis," *IEEE Trans. on Power Del.*, Vol.14, No.2, pp.561-566, Apr. 1999.

[23] J. Arrillaga, N. R. Watson, and S. Chen, *Power System Quality Assessment*, John Wiley & Sons, New York, 2000.

[24] G. W. Chang and C. I Chen, "A comparative study of voltage flicker envelope estimation methods," in *Proc. of IEEE Conference on Power and Energy Society General Meeting - Conversion and Delivery of Electrical Energy in the 21st Century*, pp. 1-6, 2008.

[25] N. Kose, O. Salor and K. Leblebicioglu, "Kalman filtering based approach for light flicker evaluation of power systems," *IET Generation, Transmission & Distribution*, Vol. 5, No. 1, pp. 57-69, Jan. 2011.

[26] H. Song, R. Na, and R. Zheng, "An advanced method for detection of instantaneous voltage flicker based on Prony analysis and Hilbert transform," *Electrical Measurement and Instrumentation*, Vol. 44, pp. 11-14, Sep. 2007.

[27] B. Widrow and M. A. Lehr, "30 years of adaptive neural networks: perceptrons," *in Proc. of IEEE*, Vol.78, No. 9, pp. 1415-1442, 1990.

[28] M. I. Marei, E. F. El-Saadany, and M. M. A. Salama, "Estimation techniques for voltage flicker envelope tracking," *Electric Power Systems Research*, Vol.70, No.1, pp. 30-37, Jun. 2004.

[29] J. Kennedy and R. Eberhart, "Particle swarm optimization," in *Proc. IEEE International Conference on Neural Networks*, Vol. 4, pp. 1942 -1948, 1995.

[30] N. M Jothi Swaroopan and P. Somasundaram, "A novel combined economic and emission dispatch control by hybrid particle swarm optimization technique," *Majlesi Journal of Electrical Engineering*, Vol. 4, No. 2, pp. 19-24, Jun. 2010.

[31] A. Sloss, D. Symes, and C. Wright, *ARM System Developer's Guide: Designing and Optimizing System Software*, Morgan Kaufmann, 2004.

Payman Moallem was born in 1970, in Tehran, Iran. He is an Associate Professor in the Department of Electrical Engineering, University of Isfahan, Iran. He received his B.S. and M.S. both in Electronics Engineering from the Isfahan University of Technology and the Amirkabir University of Technology, Iran, in 1992 and 1995, respectively. He also received his PhD in Electrical Engineering from the Amirkabir University of Technology in 2002. From 1994 to 2002, he conducted research for the Iranian Research Organization, Science and Technology (IROST) on topics like, parallel algorithms and hardware used in image processing, DSP based systems and robot stereo vision. His interests include artificial intelligence, neural networks, pattern recognition, image processing and analysis. He has published more than 50 journal papers and 100 conference papers.

Abolfazl Zargari was born in 1984, in Khomeinishahr, Iran. He received his B.S. and M.S. both in Electronic Engineering from the University of Isfahan, Iran, in 2007 and 2010, respectively. His interests include artificial intelligence, neural networks and power quality.

Arash Kiyoumarsi was born in Shahr-e-Kord, Iran, on September 11th, 1972. He received his B.Sc. (with honors) in Electronic Engineering from the Petroleum University of Technology (PUT), Iran, in 1995 and his M.Sc. and Ph.D. in Electrical Power Engineering from the Isfahan University of Technology (IUT), Iran, in 1998 and 2004, respectively. In March 2005 he joined the University of Isfahan, Faculty of Engineering, Department of Electrical Engineering as an Assistant Professor. He was a Post-Doctorate Research Fellow with the Alexander von Humboldt Foundation at the Institute of Electrical Machines, Technical University of Berlin from February to October 2006 and from July to August 2007. His research interests have included the application of finite element analysis in electromagnetics, interior permanent-magnet synchronous motor drives and applied non-linear control of electrical drives.